Preprint Cambridge Centre for Computational Chemical Engineering ISSN 1473 – 4273

Extended First-Principles Thermochemistry for the Oxidation of Titanium Tetrachloride

Philipp Buerger[1], Jethro Akroyd[1]
and Markus Kraft[1,2]

released: 03 February 2017

[1] Department of Chemical Engineering
and Biotechnology
University of Cambridge
New Museums Site
Pembroke Street
Cambridge, CB2 3RA
United Kingdom
E-mail: mk306@cam.ac.uk

[2] School of Chemical and
Biomedical Engineering,
Nanyang Technological University,
62 Nanyang Drive,
Singapore 637459

Preprint No. 180

UNIVERSITY OF CAMBRIDGE

Keywords: titanium dioxide, titanium tetrachloride, thermochemistry, thermochemical data, species generator, thermochemistry calculations, electronic structure theory, electronic structure calculations, error-cancelling balanced reactions

Edited by
Computational Modelling Group
Department of Chemical Engineering and Biotechnology
University of Cambridge
New Museums Site
Pembroke Street
Cambridge CB2 3RA
United Kingdom

Fax: + 44 (0)1223 334796
E-Mail: c4e@cam.ac.uk
World Wide Web: http://como.ceb.cam.ac.uk/

Abstract

A detailed first-principles investigation of the gas-phase precursor chemistry of titanium tetrachloride ($TiCl_4$) in an O_2 environment is used to identify the thermodynamically most stable oxidation products. Candidate species are systematically proposed based on twelve manually defined base moieties in combination with possible functional groups attached to each moiety. The ground state geometry and vibrational frequencies for each candidate species are calculated using density functional theory at the B97-1/6-311+G(d,p) level of theory. A set of 2,328 unique candidate species are found to be physically reasonable. Their thermochemical data are calculated by applying statistical thermodynamics. Standard enthalpies of formation are estimated, if unknown, by using a set of error-cancelling balanced reactions. An equilibrium composition analysis of a mixture of $TiCl_4/O_2$ (50 mol%) at 3 bar is performed to identify the thermodynamically stable products. At low temperatures, below approximately 700 K, trimer species are dominant. This is followed by a mid-temperature range of 700 to 1975 K where Ti_2OCl_6 is the most abundant species, before its thermodynamic stability decreases. Between 1200 and 1825 K $TiCl_4$ is the most stable monomer. At temperatures above 1975 K $TiOCl_2$ becomes the dominant species. This species has been measured experimentally. A structural analysis is used to suggest further potentially stable higher polymers and defines a starting point to investigate the mechanisms leading to the formation of titanium dioxide (TiO_2) particles.

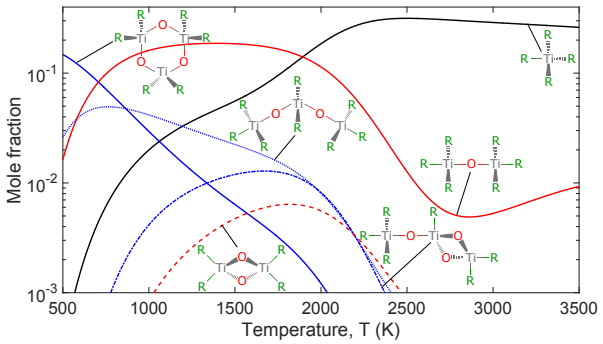

Highlights:

- First-principles calculations used to propose set of $TiCl_4$ oxidation products.
- Informed estimates of the standard enthalpy of formation calculated using multiple error-cancelling balanced reactions.
- Equilibrium composition analysis performed to identify thermodynamically stable products.
- Trimer species are dominant below 700 K.
- Mixture of monomers, dimers and trimers are thermodynamically stable between 500 and 3500 K.
- The monomer $TiOCl_2$ is the most abundant species above 1975 K.

Contents

1 Introduction **3**

2 Candidate Species Generation **4**

2.1 Algorithm and Base Moieties 4

2.2 Results 6

3 Electronic Structure Calculations **7**

3.1 Geometry Optimisations and Frequency Calculations 7

3.2 Results 7

4 Thermochemistry Calculations **9**

4.1 Partition Functions 9

4.2 Enthalpy Correction 9

4.3 Results 10

4.3.1 Cross-Validation of the Enthalpy of Formation 10

4.3.2 Calculation of the Enthalpy of Formation 11

4.3.3 Thermochemistry 11

5 Equilibrium Composition Analysis **12**

6 Mechanistic Considerations **15**

7 Conclusions **15**

References **18**

1 Introduction

Titanium dioxide (TiO_2, titania) particles are mainly used as pigment or photocatalyst. In 2015 the U.S. Geological Survey estimated the annual global TiO_2 pigment production capacity at 7.2 million metric tons [54].

The chloride process [22, 45], is one of the main commercial methods used to manufacture titanium dioxide. Purified $TiCl_4$ is fed to a high temperature oxidation reactor in which TiO_2 particles are produced via a reaction with O_2. The overall stoichiometry of the process is described by

$$TiCl_4 + O_2 \longrightarrow TiO_2(s) + 2\,Cl. \tag{1}$$

Physical parameters such as size, shape, morphology and crystalline phase strongly influence the functional behaviour of the product particles and therefore their application. Improving the ability to control these properties is a key strategic capability. Various investigations have sought to develop an understanding of the underlying chemical and physical processes in an attempt to understand how to control the particle properties more efficiently.

Ghoshtagore [14] used chemical vapour deposition to investigate the surface reaction of $TiCl_4$ on single crystal silicon wafers with a TiO_2 film at 673–1120 K. The reaction was observed to display an Eley-Rideal dependence on $TiCl_4$ and O_2. The global kinetics of $TiCl_4$ oxidation in a hot wall reactor at 973–1273 K was studied by Pratsinis et al. [43]. The reaction was first-order in $TiCl_4$ and approximately zero-order in O_2 up to ten-fold excess O_2. Pratsinis and Spicer [42] inferred a rate for the gas-phase decomposition of $TiCl_4$ based on the difference between the surface growth rate [14] and the global oxidation rate [43] under the assumption of monodisperse spherical particles. They showed that surface reaction had a significant effect on the particle diameter. Later studies using more detailed population balance models draw similar conclusions [18, 33, 34, 53].

West et al. [58, 59, 60] proposed the first detailed thermodynamically consistent gas-phase kinetic model to describe the oxidation of $TiCl_4$. This model consists of 20 $Ti_xO_yCl_z$ ($x \geq 1, y \geq 0, z \geq 0$) species which were defined based on the available literature and the authors' expertise. Oxychloride species were identified as important intermediates and the main reaction pathway was suggested to proceed via $Ti_2O_2Cl_4$. Thermochemical data were estimated by density functional theory (DFT) and statistical thermodynamics. Subsequent investigations presented an updated reaction mechanism [60] and considered the role of hydrocarbon species [52] and aluminium trichloride ($AlCl_3$) additives, known to promote the formation of the rutile crystal phase [47]. By analysing the combustion of $TiCl_4$ in a methane flame it was shown that the mole fraction of H-containing Ti-species is substantial at equilibrium and therefore are likely to be important [52]. It was found that negligible quantities of Al-containing Ti-species were present at equilibrium. Consequently it was suggested that it is more likely that $AlCl_3$ acts via the particle processes to promote the formation of rutile TiO_2 particles [47].

A large number of modelling studies have assumed simplified reaction mechanisms and often a one-step mechanism [35, 39, 42, 50, 53]. In the work of Kraft and co-workers [2, 48] it was observed that the choice of inception mechanism strongly affect the simulations of Pratsinis' original experiment [43]. This is consistent with the work of Mehta et al. [30] who compared the inception behaviour of the mechanisms from Pratsinis and Spicer [42] (one-step mechanism) and West et al. [60] (detailed mechanism). They showed that the choice of inception model caused particle inception to occur at different locations in simulations of a turbulent flame. Recently Mehta et al. [31] proposed a reduced version of the West et al. [60] mechanism to describe the oxidation of $TiCl_4$ in simulations of turbulent methane flames suitable to be coupled with computational fluid dynamics.

An accurate prediction of particle properties must consider the coupling between the gas- and particulate phase. Without consideration of the gas-phase kinetics influencing the rate of nucleation and surface growth, significant approximations have to be made affecting the quality of the model and the level of predictability that should be expected from the results.

The purpose of this work is to extend the work of West et al. [58] to perform a systematic identification of the species and to determine thermodynamically stable products present during the $TiCl_4$ oxidation. Possible products are identified and their molecular and thermodynamic properties are calculated. Equilibrium composition analysis is used to identify the subset of thermodynamically stable species.

2 Candidate Species Generation

An algorithm is presented which allows the systematic identification of possible titanium-containing products created during the oxidation of $TiCl_4$. It makes use of a set of base moieties (molecules without their functional groups) in combination with possible functional groups to propose a set of candidate species.

2.1 Algorithm and Base Moieties

A set of titanium-containing base moieties are specified as input to the algorithm. The moieties contain sub-valent sites to which functional groups can be attached. The full set of moieties used in this work is shown in Figure 1. Species containing one titanium centre are addressed as monomers, those with two titanium centres as dimers and those with three titanium centres as trimers. Monomers with coordination numbers of four, five and six and for dimers and trimers only a coordination number of four were considered.

The algorithm systematically combines the moieties with possible functional groups to generate a set of candidate species. The functional groups $-$OCl, $-$O and $-$Cl as well as a possible sub-valent sites were considered in the algorithm. Duplicates were identified using a molecular description, for example InChI [20, 28] or SMILES [38, 56, 57], and were rejected. An illustration of the algorithm for two different species is given in Figure 2.

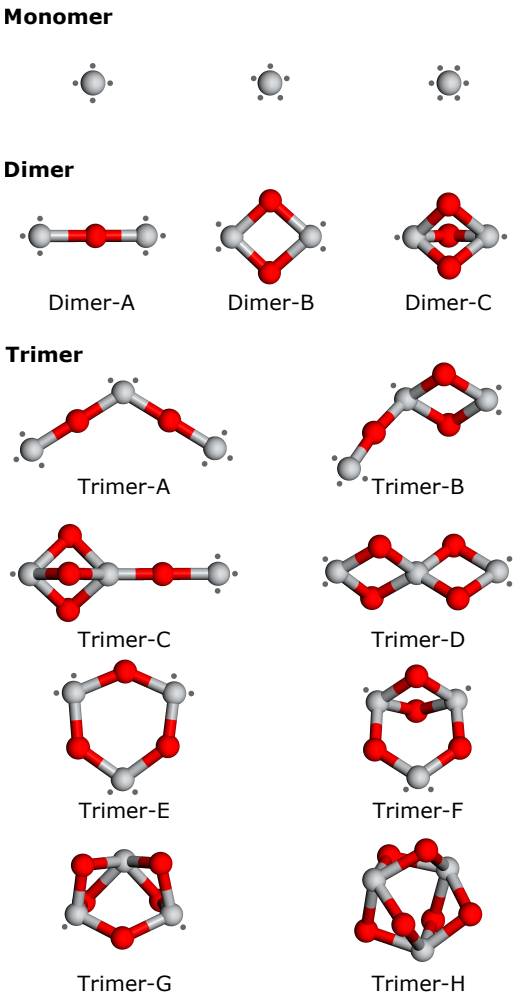

Figure 1: *Manually defined base moieties consisting of atomic titanium (grey), oxygen (red) and sub-valent sites (.). Functional groups are able to be attached to the sub-valent sites.*

This algorithm is also applicable for titanium species containing titanium atoms with higher coordination numbers. Hence, in this work monomers with coordination numbers of five and six were also considered. In addition, $Ti_2O_2Cl_5$ (in this work labelled as $Ti_2O_2Cl_5-3$), $Ti_2O_2Cl_6$ (in this work labelled as $Ti_2O_2Cl_6-2$) and $Ti_5O_6Cl_8$ were considered by West et al. [58, 60] and are included for the purpose of comparison.

The effect of spin multiplicity on the ground states of the titanium-containing species derived from titanium tetraisopropoxide (TTIP, $Ti(OC_3H_7)_4$) [6] was analysed. It was observed that bonds between two $-O$ groups can increase the stability of a species. The algorithm automatically identifies the combinations of functional groups that could lead to such intramolecular interactions and a separate candidate species is generated for each such case. The original species without any functional group interactions also remains within the set. In this work only $O-O$ interactions were considered.

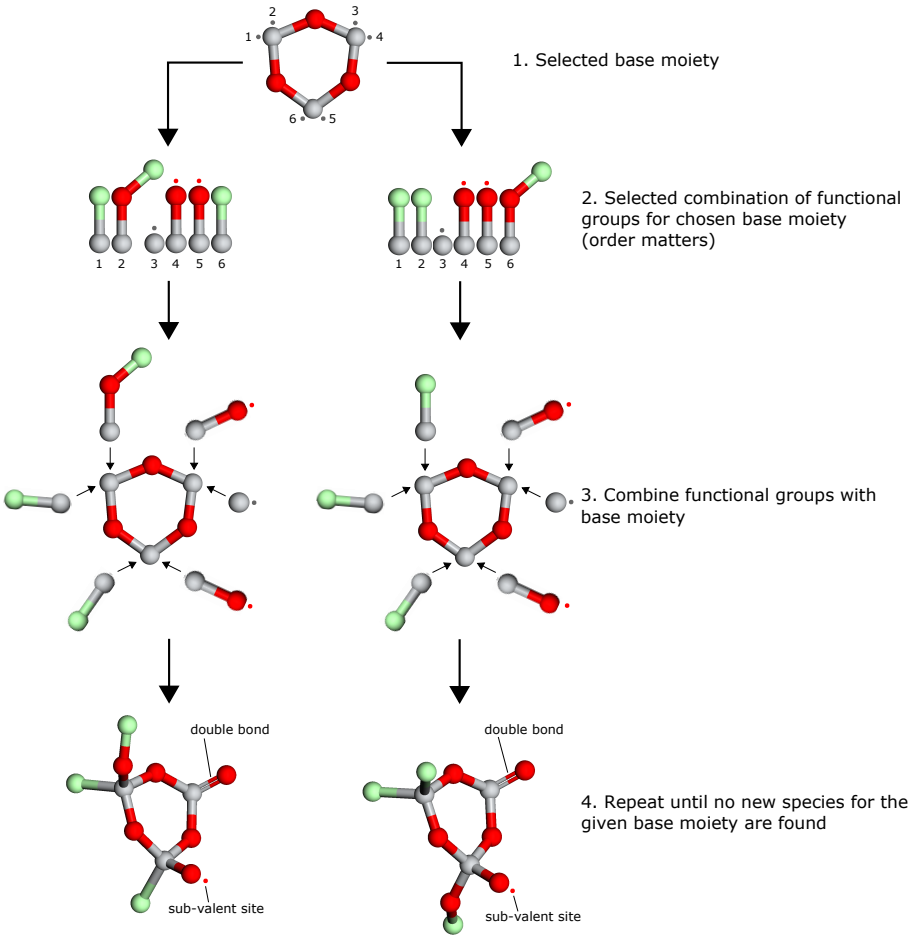

Figure 2: *Principle of the species generation algorithm for a selected base moiety and two combinations of functional groups.*

The structural families in this paper are defined by classifying each candidate species by its base moiety. For example, all species containing two titanium atoms connected by two oxygen atoms is a member of the structural family Dimer-B.

2.2 Results

An initial set of $119,148$ $Ti_xO_yCl_z$ ($1 \leq x \leq 3, y \geq 0, z \geq 0$) species was generated, of which $5,543$ unique species remained after rejecting duplicates. In order to keep the set at a manageable size, species with more than three Ti atoms were not considered due to the combinatorial increase in the number of species.

It was assumed that species with more than one radical site are likely to be short-lived. Trimers with more than one radical site were rejected. Radical monomers and dimers with more than one radical site were kept under the assumption that they may be important in the initial stages of the gas-phase precursor chemistry and are therefore required for kinetic mechanism development. This reduced the set of candidate species to a total of $2,436$ unique species.

3 Electronic Structure Calculations

3.1 Geometry Optimisations and Frequency Calculations

Geometry optimisation and frequency calculations were performed using density functional theory (DFT) at the B97-1/6-311+G(d,p) level of theory for each of the 2,436 candidate species. The B97-1 hybrid functional has previously been shown to be accurate [5, 16] and well suited for transition metal complexes [13, 23, 51]. Scaling factors were used as proposed by Merrick et al. [32] to compensate for the overestimation of the calculated harmonic frequencies

The Gaussian09 software package [12], running on Intel(R) Xeon(R) CPU X5472 @ 3GHz/ 8GB nodes with 8 cores per node, was used to perform all electronic structure calculations. A tight convergence criterion and an ultrafine (99,590) pruned grid were chosen. The calculations were set to distinguish between open- and closed-shell species. Analysing the effect of the spin multiplicity on the calculated ground states of species derived from TTIP [6] showed that it was valid to select the spin multiplicity based on the number of sub-valent sites for each species.

The initial guess of the geometry for each candidate species was extracted from the optimised ground state geometry of the largest species in the structural family. In this work, the largest species is formed from the base moiety with only $-$OCl functional groups attached. These species were step-wise optimised, building the molecule atom-by-atom from the base moiety, re-optimising the structure after adding each layer of new atoms. This reduces the overall optimisation problem to a set of smaller problems. Each optimisation step is started from a near-optimal geometry with the aim to increase the likelihood of finding the global minimum.

The ground state geometries of multiple conformers were calculated for species showing high degrees of freedom. This mainly includes candidate species of the families Dimer-A and Trimer-A. Also in cases were the geometry optimisation failed to converge, multiple manually defined geometries were used as initial guesses.

In several cases, initially distinct candidate species converged to the same structure. The duplicates were identified using canonical SMILES as implemented in OpenBabel [38] and were removed from the species set. Only the lowest energy conformer was retained.

3.2 Results

The ground state geometries and vibrational frequencies were calculated for all candidate species. It was verified that no imaginary frequencies were present. The optimised ground state geometries of key species are presented in Figure 3.

It was observed that some structural families seem to be more physically reasonable than others. For example, the convergence of an initial Dimer-A type geometry into a Dimer-B type geometry, indicating that double oxygen bridges are favoured over radical oxygen groups. Another observation was that the cyclic structures (Trimer-E and Trimer-F) seemed to be more reasonable than the non-cyclic ones. In particular

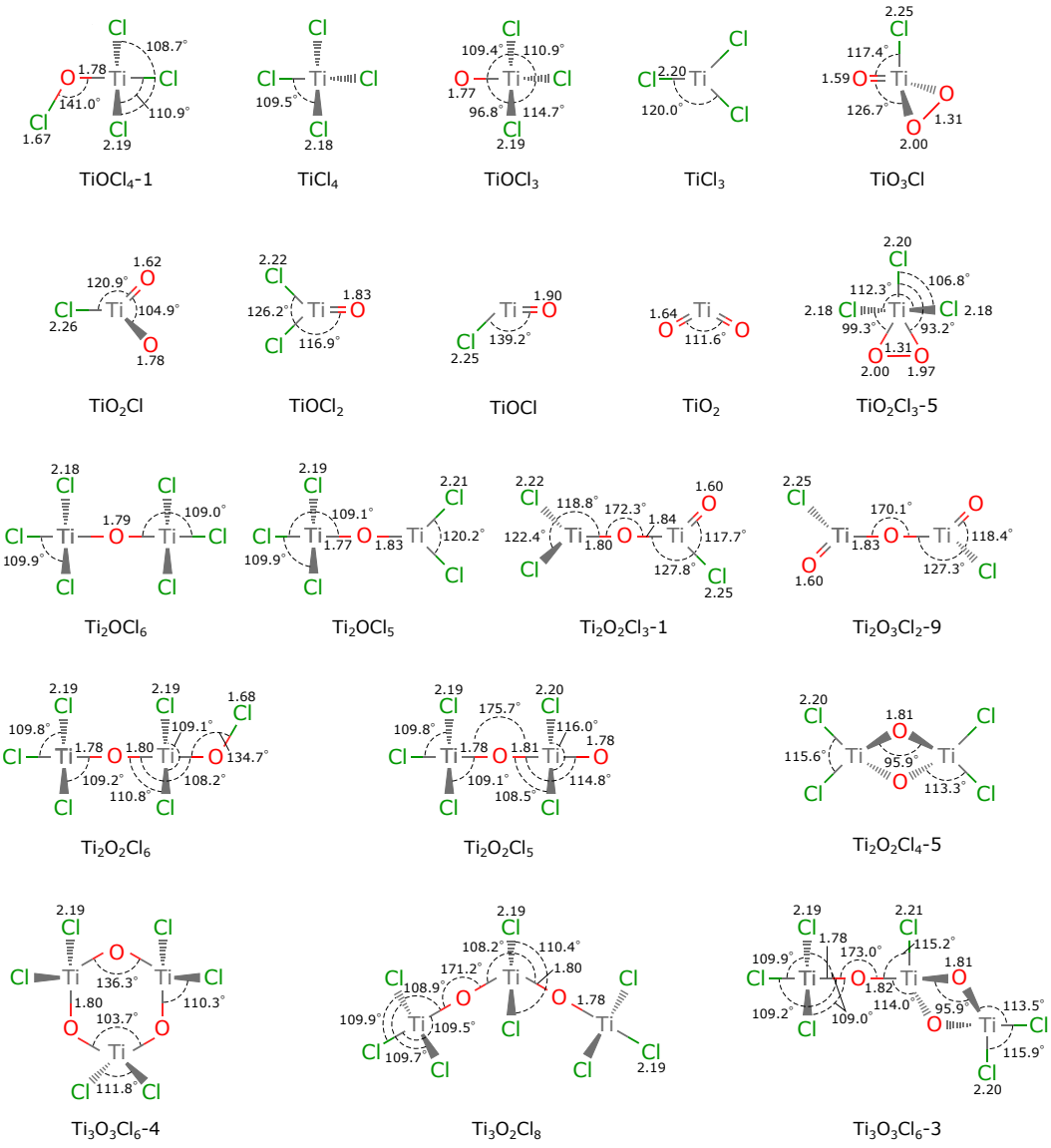

Figure 3: *Optimised ground state geometries for key species calculated at the B97-1/6-311+G(d,p) level of theory. Bond lengths are reported in Ångströms.*

Trimer-A and Trimer-B type species often converged into more compact cyclic or bent unclosed-cyclic structures.

After removing duplicates, the final set of candidate species with optimised ground state geometries and calculated scaled frequencies contained 2,328 unique titanium-containing species.

4 Thermochemistry Calculations

4.1 Partition Functions

Statistical thermodynamics was used to calculate the heat capacity, entropy and enthalpy of each species for the temperature range $200 - 4000$ K. Translational, vibrational, rotational and electronic energy contributions were considered. For the treatment of the translational and rotational motion the standard classical approximation was used. For the vibrational motions a simple harmonic-oscillation approximation was applied. This has been previously shown to be sufficient for a TTIP-based set of titanium containing species [6]. It was assumed that only the ground state is accessible, which reduces contributions from the electronic mode to the spin multiplicity (1 for non-radical species). Details about partition function calculations can be found in a number of textbooks [29, 46]. The calculation method has previously been validated against hydrocarbons and showed very good agreement with available experimental data [6].

4.2 Enthalpy Correction

The partition functions allow the calculation of the enthalpy change,

$$\Delta H^\circ(T) = H^\circ(T) - \Delta_f H^\circ_{0\,\mathrm{K}} \tag{2}$$

where the standard enthalpy of formation at 0 K, $\Delta_f H^\circ_{0\,\mathrm{K}}$, is required for the calculation of the absolute enthalpy $H^\circ(T)$. Assuming the standard ambient temperature of 298.15 K, equation (2) can be rewritten as

$$\Delta H^\circ(298.15\ \mathrm{K}) = \Delta_f H^\circ_{298.15\,\mathrm{K}} - \Delta_f H^\circ_{0\,\mathrm{K}}. \tag{3}$$

Given the standard enthalpy of formation, $\Delta_f H^\circ_{298.15\,\mathrm{K}}$, and the enthalpy change, $\Delta H^\circ(298.15\ \mathrm{K})$, equation (3) can be solved for $\Delta_f H^\circ_{0\,\mathrm{K}}$ and equation (2) for $H^\circ(T)$.

The standard enthalpy of formation is not always known experimentally or theoretically. In the case of species where data was not available, the concept of error-cancelling balanced reactions (EBRs) was used to obtain an estimate of the standard enthalpy of formation. By applying Hess' Law, the enthalpy of formation of one of the species in an EBR can be calculated based on knowledge of the enthalpies of formation of the other species in the reaction. This method requires knowledge of the total electronic energy for each species in the EBR and the standard enthalpies of formation for all except the species for which the enthalpy is being calculated.

The *isodesmic* and *isogyric* reaction classes were used in this work [17, 40, 41]. Isogyric reactions conserve the number of spin pairs, whilst isodesmic reactions conserve the bond types between two atoms on either side of the reaction, such that systematic errors inherited from the electronic structure calculations approximately cancel out. The choice of the reaction has an effect on the accuracy of the estimate of the standard enthalpy of formation. For this reason, a set of EBRs was used

from which an average value of the enthalpy of formation was calculated. This has been shown to significantly improve the accuracy of the method and additionally provides an estimate of the uncertainty in the results [7, 9].

The reference data for the standard enthalpies of formation used in this work are listed in Table 1. Absolute differences between literature data of up to 94.4 kJ mol^{-1} were found for the oxychloride species. The effect of the reference data (Table 1) on the accuracy of the method is assessed using a cross-validation technique. The method is described in full elsewhere [7, 9] and is summarised here. The standard enthalpy of formation is iteratively estimated for each species in the reference set, assuming that the enthalpy of the species under investigation is unknown. The estimated value was then compared against the reference value and an accuracy metric assigned to the data [7, 9]. The cross-validation was used to identify and avoid the use of unreliable reference data. The data in Table 1 are the final post cross-validation reference data that were used in this work.

Table 1: *Reference data for enthalpies of formation for relevant species.*

species	$\Delta_f H^\circ_{298.15\,K}$ [kJ mol^{-1}]	species	$\Delta_f H^\circ_{298.15\,K}$ [kJ mol^{-1}]
Ti-containing species		*Other species*	
$TiCl_4$	−763.16 [10, 27]	ClO	101.63 [1, 3, 4, 10, 27]
$TiCl_3$	−508.36 [19]	ClO_2	98.00 [10, 27]
$TiCl_2$	−205.02 [19]	ClO_3	201.00 [44]
TiCl	171.13 [19]	ClO_4	229.28 [49]
$TiOCl_2$	−593.29 [55]	OClO	94.60 [4, 10, 11, 27, 36]
TiOCl	−286.85 [7]	Cl_2	0.00 [10, 27]
TiO_2	−305.43 [10, 27]	ClOCl	82.80 [1]
TiO	54.39 [10, 27]	Cl_2O	90.00 [10, 27]
		Cl_2O_2	154.20 [10, 24, 25, 27]
		Cl_2O_3	137.00 [1]
		Cl_2O_4	186.10 [26]
		Cl_2O_5	258.30 [26]
		Cl_2O_6	278.50 [26]
		Cl_2O_7	321.30 [26]
		ClOClO	175.50 [10, 25, 27]
		ClOOCl	133.00 [1]
		O_2	0.00 [10, 27]

4.3 Results

4.3.1 Cross-Validation of the Enthalpy of Formation

The cross-validation of the reference species (Table 1) was performed separately using isodesmic and isogyric reaction. A mean absolute error of 11.71 kJ mol^{-1} was obtained using isodesmic reactions and 48.36 kJ mol^{-1} using isogyric reactions. In addition, the mean absolute error was also calculated separately for titanium-containing species. The mean absolute error for titanium-containing species was 2.86 kJ mol^{-1} for isodesmic reactions and 19.64 kJ mol^{-1} for isogyric reactions.

The larger error for isogyric reactions is not unexpected because this reaction class is far less restrictive than isodesmic reactions. These errors are deemed to be accept-

able given the uncertainties of the reference data that are used in the calculations (Table 1).

4.3.2 Calculation of the Enthalpy of Formation

The enthalpy of formation of the candidate species was calculated using isodesmic reactions wherever possible. However, the small number of species for which reference data was available meant that isogyric reactions had to suffice for most species. A larger set of titanium-containing reference species would enable the use of more isodesmic reactions and lead to lower uncertainties in the estimated standard enthalpies.

The calculations in this work do not rely on a single EBR, but use a set of EBRs for each species. This has been shown to significantly improve the accuracy of calculations based on EBRs [7, 9], providing some compensation from the use of isogyric reactions.

The two largest discrepancies between the enthalpy estimates of West et al. [58] and those calculated here are for $Ti_2O_3Cl_3$ and TiO_2Cl_2. A set of 12 isogyric reactions were used for $Ti_2O_3Cl_3$ and 17 reactions for TiO_2Cl_2. A value of -1086.81 ± 47.68 kJ mol^{-1} compared to -1418.00 kJ mol^{-1} was determined for $Ti_2O_3Cl_3$ and -626.52 ± 18.48 kJ mol^{-1} compared to -558.00 kJ mol^{-1} for TiO_2Cl_2. None of the calculated isogyric reactions for $Ti_2O_3Cl_3$ were close to the value of -1418.00 kJ mol^{-1} [58], which was estimated using a single anisogyric reaction. The closest and largest value for TiO_2Cl_2 observed within the distribution was -589.63 kJ mol^{-1}. For all other species, the enthalpy estimates published by West et al. [58, 60] are in acceptable agreement with this work.

4.3.3 Thermochemistry

The calculated thermochemical data are in excellent agreement with those proposed by West et al. [58]. Thermochemical data for key titanium-containing species are reported in Table 2. In addition, the calculated thermochemical data for the full set of candidate species are provided as supporting information.

Table 2: *Thermochemical data for $TiCl_4$ and selected oxidation products. Where available, reference data for the standard enthalpies of formation were taken from the literature.*

species	$\Delta_f H^\circ_{298.15\,K}$	$S^\circ_{298.15\,K}$	C_p [J mol^{-1} K^{-1}]						
	[kJ mol^{-1}]	[J mol^{-1} K^{-1}]	300	500	1000	1500	2000	2500	3000
Monomer									
Cl_4Ti	-763.16 [10, 27]	355.66	96.17	103.43	106.82	107.51	107.78	107.87	107.94
Cl_4OTi-1	-759.44	422.66	114.43	124.68	130.61	131.92	132.43	132.62	132.73
Cl_3Ti	-508.36 [19]	340.24	75.27	80.07	82.30	82.76	82.94	83.00	83.04
Cl_3OTi	-635.15[a]	375.51	95.01	102.69	106.59	107.41	107.73	107.84	107.91
Cl_3O_2Ti-5	-766.44[b]	402.17	111.01	122.32	129.69	131.47	132.18	132.44	132.61
Cl_2OTi	-593.29 [55]	337.51	70.31	76.53	81.08	82.18	82.62	82.78	82.88
$ClOTi$	-286.88 [7][c]	292.45	49.34	53.34	56.66	57.48	57.81	57.93	58.01
ClO_2Ti	-493.01	318.34	70.23	76.84	81.26	82.27	82.67	82.82	82.91
ClO_3Ti	-673.42	340.24	83.58	94.78	103.79	106.06	106.97	107.32	107.54
O_2Ti	-305.44 [10, 27]	260.15	44.22	50.40	55.74	57.04	57.60	57.86	58.13
Dimer									
Cl_6OTi_2	-1587.38	562.33	180.56	196.41	204.64	206.39	207.08	207.32	207.47
$Cl_6O_2Ti_2$	-1593.33	609.58	198.78	217.72	228.48	230.82	231.74	232.06	232.27
Cl_5OTi_2	-1333.63	543.83	159.78	173.09	180.14	181.65	182.24	182.45	182.58
$Cl_5O_2Ti_2$	-1471.18	571.99	179.30	195.64	204.41	206.29	207.02	207.27	207.44
$Cl_4O_2Ti_2-5$	-1540.83[d]	451.87	149.84	168.50	178.86	181.06	181.92	182.23	182.42
$Cl_3O_2Ti_2-1$	-1167.29	501.18	133.73	146.14	154.40	156.32	157.08	157.35	157.53
$Cl_2O_3Ti_2-9$	-1217.59	471.20	128.39	142.51	153.17	155.73	156.75	157.13	157.37
Trimer									
$Cl_6O_3Ti_3-3$	-2362.12	657.17	234.08	261.43	276.67	279.94	281.21	281.66	281.96
$Cl_6O_3Ti_3-4$	-2427.37	607.87	235.31	262.23	276.90	280.05	281.27	281.71	281.99
$Cl_8O_2Ti_3$	-2411.29	740.58	264.80	289.38	302.47	305.28	306.37	306.76	307.01

[a] West et al. [58] reported a value of -639.00 kJ mol^{-1}.
[b] West et al. [58] reported a value of -774.00 kJ mol^{-1}.
[c] West et al. [58] reported a value of -274.00 kJ mol^{-1}.
[d] West et al. [58] reported a value of -1552.00 kJ mol^{-1}.

5 Equilibrium Composition Analysis

Equilibrium composition analysis was used to identify the thermodynamically stable $TiCl_4$ oxidation products. Figure 4 presents the calculated equilibrium composition for an initial mixture of $TiCl_4/O_2$ (50 mol%) at 3 bar for a temperature range of $500-3500$ K, where each point on the graph was calculated at constant pressure and temperature. The full set of 2,328 $Ti_xO_yCl_z$ candidate species plus 20 O_yCl_z ($y \geq 0, z \geq 0$) species were included in the calculation. The calculations were performed using Cantera [15]. The thermochemical data for O, O_2, O_3, Cl, Cl_2 and Ti were taken from the database provided with Cantera [15]. Thermochemical data for all other species considered in this work were calculated as per sections 3 and 4.

The titanium-containing species in Figure 4 are all present at high mole fractions. This includes $TiOCl_2$, Ti_2OCl_6, $Ti_3O_3Cl_6-4$, $TiCl_4$, $Ti_3O_2Cl_8$, $Ti_3O_3Cl_6-3$, $Ti_2O_2Cl_4-5$, $TiOCl$, TiO_2Cl, $TiCl_3$, $Ti_2O_2Cl_3-1$, $Ti_2O_3Cl_2-9$, $TiOCl_4-1$, TiO_2, $Ti_2O_2Cl_6$, $Ti_2O_2Cl_5$, TiO_3Cl, $TiOCl_3$, TiO_2Cl_3-5 and Ti_2OCl_5. The optimised ground state geometries for these species are shown in Figure 3.

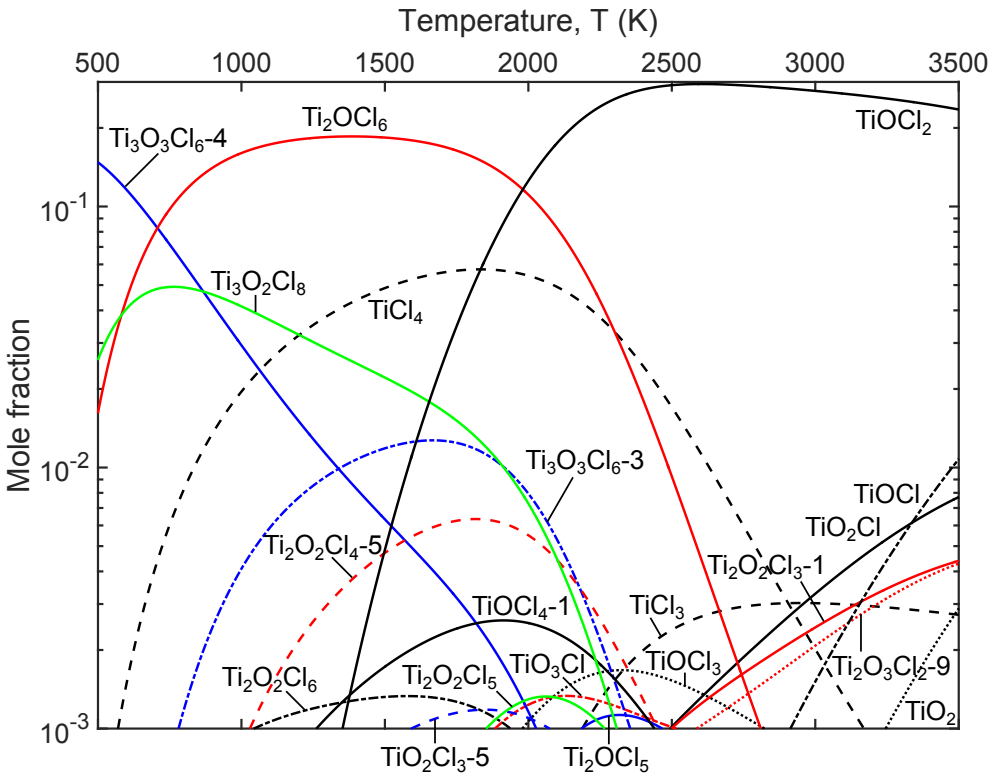

Figure 4: *Calculated equilibrium composition as a function of temperature for an initial mixture of $TiCl_4/O_2$ (50 mol%) at 3 bar. Only titanium-containing species are shown. Optimised ground state geometries for these species are presented in Figure 3.*

Trimer species are found to be most stable at low temperatures, below approximately 700 K. The main trimer species are $Ti_3O_3Cl_6-4$ and $Ti_3O_2Cl_8$. The titanium atoms in these species are connected by single oxygen atoms (single oxygen bridges). Above 700 K, the Ti_2OCl_6 dimer becomes dominant up to 1975 K. This also contains a single oxygen bridge. In addition, there are stable species with titanium atoms connected by two oxygen atoms (double oxygen bridges) in this temperature range. This includes $Ti_2O_2Cl_4-5$ and $Ti_3O_4Cl_4-7$. A rapid increase in the thermodynamic stability of $TiOCl_2$ is observed above 1400 K. This species has also been observed experimentally [21] and becomes the most thermodynamically stable species above 1975 K. The $TiCl_4$ precursor is present at notable mole fractions at temperatures between 1200 and 1825 K. Its thermodynamic stability significantly decreases at high temperatures. The geometries of all of these species are shown in Figure 3. Only low mole fractions of the dimers $Ti_2O_2Cl_6-2$ (labelled $Ti_2O_2Cl_6$ by West et al. [60]) and $Ti_2O_2Cl_5-3$ (labelled $Ti_2O_2Cl_5$ by West et al. [60]), which possess titanium atoms with coordination numbers of five, were observed. Across the full temperature range, other monomers with a coordination number of five or six were not stable.

The mole fractions of radical species such as TiOCl or TiO_2Cl are observed to increase with increasing temperature. Out of the species shown in Figure 4 only $TiOCl_4-1$ and $Ti_2O_2Cl_6$ were found to have an OCl functional group. Across all candidate species it was observed that the thermodynamically more stable species typically have fewer $-$OCl

functional groups.

A significant degree of agreement is found with the work of West et al. [58], where species such as $TiOCl_2$, $TiCl_4$, TiO_2Cl_3 (in this work labelled as TiO_2Cl_3-5) and $Ti_2O_2Cl_4$ (in this work labelled as $Ti_2O_2Cl_4-5$) were found to be stable. Some differences are also observed. The mole fractions of the single trimer $Ti_3O_4Cl_4$ (in this work labelled as $Ti_3O_4Cl_4-6$) and pentamer $Ti_5O_6Cl_8$ considered by West et al. [58] are found to be significantly lower in this work. Such differences are to be expected because of the significantly extended species pool that was able to be considered in this work.

Figure 5a summarises the equilibrium data in terms of monomers, dimers and trimers. As expected, larger polymers (trimers) are found to be thermodynamically most stable at lower temperatures below 700 K and their stability decreases with increasing temperature. It is observed that dimers are the thermodynamically most stable species group at temperatures between approximately 700 and 1975 K. The thermodynamic stability of monomers gradually increases with temperature and they are dominant at temperatures approximately above 1975 K.

Figure 5b shows the species mole fractions grouped by their structural family (Figure 1). The most abundant structural family at temperatures below 700 K is Trimer-E. This contains cyclic species with single oxygen bridges. A rapid decrease in the thermodynamic stability of Trimer-E species is observed with increasing temperature. The Trimer-A and Trimer-B families are also observed at significant mole fractions. Both contain non-cyclic species. Trimer-A species contains single oxygen bridges. Trimer-B species contain both a single and double oxygen bridge. The Dimer-A family is dominant at temperatures between 700 and 1975 K. This contains species with single oxygen bridges. The Dimer-B family is also observed but at lower mole fractions. Over the full temperature range, Dimer-A was found to be thermodynamically more stable than Dimer-B. At temperatures above 1975 K, monomer species are most stable.

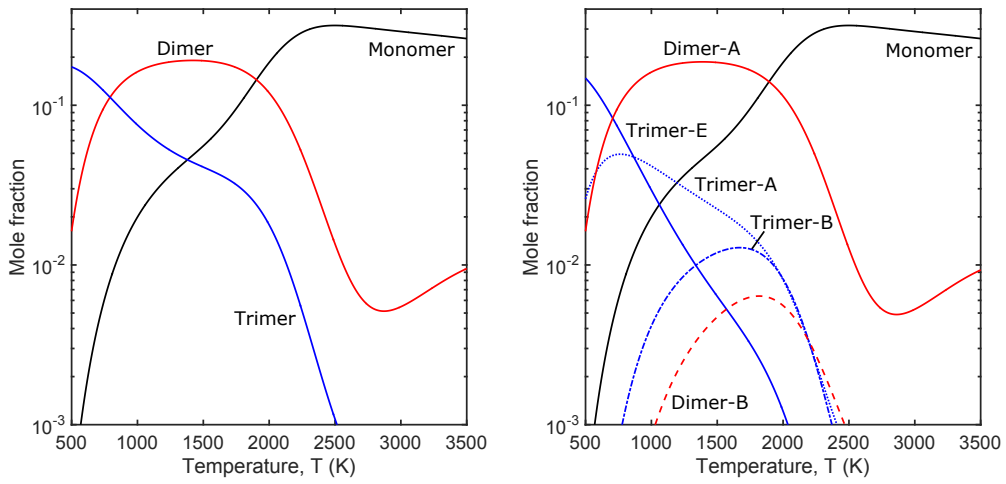

(a) *Grouped species as monomers, dimers and trimers.*

(b) *Structural families as defined in Figure 1.*

Figure 5: *Summary of species groups.*

The structural analysis is useful to suggest further potentially stable higher polymers, whilst

keeping the set of candidate species at a manageable size, rather than considering a combinatorially increasing number of species. This gives a starting point to investigate the mechanisms leading to the formation of TiO_2 particles.

6 Mechanistic Considerations

It is possible to gain some mechanistic insight based on the equilibrium composition analysis, presented in section 5, and the existing reaction mechanism [59, 60].

Ti_2OCl_6 could be the product of a bimolecular reaction between $TiCl_3$ and $TiOCl_3$. Other pathways producing Ti_2OCl_6 are also possible and would need to be considered. In the mechanism proposed by West et al. [59, 60], $TiOCl_3$ is an essential intermediate on pathways to TiO_2Cl_4-5. It is assumed that $TiOCl_3$ may also be an important intermediate on pathways involving Ti_2OCl_6.

Depending on the temperature, $Ti_3O_2Cl_8$ could perhaps be involved in pathways that include Ti_2OCl_6 and $TiOCl_3$, $Ti_2O_2Cl_5$ and $TiCl_3$, and Ti_2OCl_5 and $TiOCl_3$. The abstraction of a chlorine atom from $Ti_2O_2Cl_5$ followed by an internal restructuring could lead to $Ti_2O_2Cl_4-5$. A similar internal restructuring of $Ti_2O_2Cl_5$ might also produce $Ti_2O_2Cl_5-3$. Both $Ti_2O_2Cl_4-5$ and $Ti_2O_2Cl_5-3$ were found to be important and are discussed in detail by West et al. [58, 59, 60].

This is certainly not a complete list and is not the focus of this work. Many other pathways may need to be considered. One way to approach this problem systematically could be to define reaction rules for the functional groups in each structural family. This would enable the automatic generation of an initial mechanism, analogous to previous investigations of tetraethoxysilane (TEOS) [37] and titanium tetraisopropoxide (TTIP) [8]. The mechanism could then be refined iteratively.

7 Conclusions

An extended first-principles investigation of the gas-phase precursor chemistry of $TiCl_4$ in an O_2 environment was conducted using quantum chemistry, statistical thermodynamics and equilibrium composition analysis. A simple rigid-rotor harmonic-oscillator approximation was assumed. Thermochemical data for a large set of possible Ti−O−Cl species were calculated and analysed.

Possible candidate species, which could be present during the reaction of $TiCl_4$, were systematically identified. Species with up to three titanium atoms were considered, including monomer species with coordination numbers of four, five and six. Trimer species with more than one radical site were assumed to be short-lived and excluded from further analysis. Monomers and dimers with multiple radical sites were assumed to be important in the initial stages of the precursor chemistry, even though they might not be thermodynamically stable, and were kept in the species pool. The algorithm used to identify the species could be extended to other polymer species following the same geometric principles. The ground state geometry and scaled harmonic vibrational frequencies were calculated using the B97-1/6-311+G(d,p) level of theory for $2,328$ unique titanium-containing candidate species.

In cases where no standard enthalpy of formation was known, a set of error-cancelling

balanced reactions was used to estimate the standard enthalpy of formation. Isodesmic reactions were preferentially used over isogyric reactions. It was found that due to the scarcity of reference data for titanium-containing species, the application of isodesmic reactions was limited and isogyric reactions had to suffice for most species. Acceptable mean absolute errors were calculated by performing a cross-validation for the titanium-containing species using each reaction class. Significant uncertainties in the calculated standard enthalpies of formation were shown to result from the necessary use of isogyric reactions and the limited set of error-cancelling balanced reactions that can be found given a small set of reference species. Additional experimental data would be beneficial in enabling the use of a wider range of balanced reaction and therefore in achieving higher accuracy estimates.

Equilibrium analysis was used to identify the thermodynamically stable titanium-containing species for an initial mixture of $TiCl_4/O_2$ (50 mol%) at 3 bar. Trimer species were found to be dominant at temperatures below 700 K. A mixture of trimers, dimers and monomers were stable between 700 to 2500 K. Ti_2OCl_6 was the most stable species between 700 and 1975 K, after which its stability decreased rapidly. At temperatures above 1975 K, $TiOCl_2$ became the dominant species.

The equilibrium composition was analysed in terms of the structural families of the species. Trimer species including both cyclic and non-cyclic structures were dominant at low temperatures. Their stability decreased with temperature. At mid-temperatures, a mixture of structural families were present. This includes trimers, dimers with a single and double oxygen bridge and monomers. The Dimer-A family (single oxygen bridge) was prevalent over the Dimer-B family (double oxygen bridge) across the full temperature range. At temperatures above 1975 K, monomers were the most stable family.

The obvious next step is to use the calculated data and observations to refine the existing gas-phase chemical mechanism leading to the formation of particles. This will require the identification of reaction pathways, using the identified thermodynamically stable species as guide. An automated reaction mechanism generator could be employed to suggest possible pathways. Reaction rules could be defined based on structural families and attached functional groups.

Acknowledgements

This project is partly funded by the National Research Foundation (NRF), Prime Minister's Office, Singapore under its Campus for Research Excellence and Technological Enterprise (CREATE) programme. The authors thank Huntsman Pigments and Additives for financial support.

Supporting Information

Thermochemical data for the $2,328$ candidate species are provided in the form of NASA polynomial coefficients in CHEMKIN format and as comma separated (.csv) files tabulating the heat capacity, entropy and absolute enthalpy as a function of temperature. The calculated standard enthalpies of formation for the candidate species, the uncertainty in the estimate and the number of error-cancelling balanced reactions used in the calculation are

available in tabulated form. An additional table mapping each species to a SMILES string is also provided. The molecular geometries are available on request.

References

[1] S. Abramowitz and M. Chase. Thermodynamic Properties of Gas Phase Species of Importance to Ozone Depletion. *Pure Appl. Chem.*, 63(10):1449–1454, 1991.

[2] J. Akroyd, A. J. Smith, R. Shirley, L. R. McGlashan, and M. Kraft. A Coupled CFD-Population Balance Approach for Nanoparticle Synthesis in Turbulent Reacting Flows. *Chem. Eng. Sci.*, 66(17):3792–3805, 2011. doi:10.1016/j.ces.2011.05.006.

[3] R. Atkinson, D. L. Baulch, R. A. Cox, R. F. Hampson, J. A. Kerr, M. J. Rossi, and J. Troe. Evaluated Kinetic and Photochemical Data for Atmospheric Chemistry, Organic Species: Supplement VII. *J. Phys. Chem. Ref. Data*, 28(2):191–393, 1999. doi:10.1063/1.556048.

[4] W. J. Bloss, S. L. Nickolaisen, R. J. Salawitch, R. R. Friedl, and S. P. Sander. Kinetics of the ClO Self-Reaction and 210 nm Absorption Cross Section of the ClO Dimer. *J. Phys. Chem. A*, 105(50):11226–11239, 2001. doi:10.1021/jp012429y.

[5] A. D. Boese, J. M. L. Martin, and N. C. Handy. The Role of the Basis Set: Assessing Density Functional Theory. *J. Chem. Phys.*, 119(6):3005–3014, 2003. doi:10.1063/1.1589004.

[6] P. Buerger, D. Nurkowski, J. Akroyd, S. Mosbach, and M. Kraft. First-Principles Thermochemistry for the Thermal Decomposition of Titanium Tetraisopropoxide. *J. Phys. Chem. A*, 119(30):8376–8387, 2015. doi:10.1021/acs.jpca.5b01721.

[7] P. Buerger, J. Akroyd, S. Mosbach, and M. Kraft. A Systematic Framework to Estimate and Validate Enthalpies of Formation Using Error-Cancelling Balanced Reactions. *In preparation*, 2016.

[8] P. Buerger, D. Nurkowski, J. Akroyd, and M. Kraft. A Kinetic Mechanism for the Thermal Decomposition of Titanium Tetraisopropoxide. *Proc. Combust. Inst., In Press*, 2016. doi:10.1016/j.proci.2016.08.062.

[9] P. Buerger, J. Akroyd, J. W. Martin, and M. Kraft. A Big Data Framework to Validate Thermodynamic Data for Chemical Species. *Combust. Flame*, 176:584–591, 2017. doi:10.1016/j.combustflame.2016.11.006.

[10] M. W. J. Chase. *NIST-JANAF Thermochemical Tables, 4th Edition*. American Institute of Physics, New York, 1998.

[11] W. B. DeMore, S. P. Sander, D. Golden, R. F. Hampson, M. J. Kurylo, C. Howard, A. Ravishankara, C. Kolb, and M. Molina. Chemical Kinetics and Photochemical Data for Use in Stratospheric Modeling. Evaluation No. 12. *J. Org. Chem.*, 1997.

[12] M. J. Frisch, G. W. Trucks, H. B. Schlegel, G. E. Scuseria, M. A. Robb, J. R. Cheeseman, G. Scalmani, V. Barone, B. Mennucci, G. A. Petersson, H. Nakatsuji, M. Caricato, X. Li, H. P. Hratchian, A. F. Izmaylov, J. Bloino, G. Zheng, J. L. Sonnenberg, M. Hada, M. Ehara, K. Toyota, R. Fukuda, J. Hasegawa, M. Ishida, T. Nakajima, Y. Honda, O. Kitao, H. Nakai, T. Vreven, J. A. Montgomery, Jr., J. E. Peralta,

F. Ogliaro, M. Bearpark, J. J. Heyd, E. Brothers, K. N. Kudin, V. N. Staroverov, R. Kobayashi, J. Normand, K. Raghavachari, A. Rendell, J. C. Burant, S. S. Iyengar, J. Tomasi, M. Cossi, N. Rega, J. M. Millam, M. Klene, J. E. Knox, J. B. Cross, V. Bakken, C. Adamo, J. Jaramillo, R. Gomperts, R. E. Stratmann, O. Yazyev, A. J. Austin, R. Cammi, C. Pomelli, J. W. Ochterski, R. L. Martin, K. Morokuma, V. G. Zakrzewski, G. A. Voth, P. Salvador, J. J. Dannenberg, S. Dapprich, A. D. Daniels, Ö. Farkas, J. B. Foresman, J. V. Ortiz, J. Cioslowski, and D. J. Fox. Gaussian 09 Revision D.01, 2009.

[13] Y. Ge, D. DePrekel, K.-T. Lam, K. Ngo, and P. Vo. Assessing Density Functionals for the Prediction of Thermochemistry of Ti − O − Cl Species. *J. Theor. Comput. Chem.*, 14(08):1550055, 2015. doi:10.1142/S0219633615500558.

[14] R. N. Ghoshtagore. Mechanism of Heterogeneous Deposition of Thin Film Rutile. *J. Electrochem. Soc.*, 117(4):529–534, 1970. doi:10.1149/1.2407561.

[15] D. G. Goodwin. An Open-Source, Extensible Software Suite for CVD Process Simulation, 2003. URL `www.cantera.org`.

[16] M. W. D. Hanson-Heine, M. W. George, and N. A. Besley. Investigating the Calculation of Anharmonic Vibrational Frequencies Using Force Fields Derived from Density Functional Theory. *J. Phys. Chem. A*, 116(17):4417–4425, 2012. doi:10.1021/jp301670f.

[17] W. J. Hehre, R. Ditchfield, L. Radom, and J. A. Pople. Molecular Orbital Theory of the Electronic Structure of Organic Compounds. V. Molecular Theory of Bond Separation. *J. Am. Chem. Soc.*, 92(16):4796–4801, 1970. doi:10.1021/ja00719a006.

[18] M. C. Heine and S. E. Pratsinis. Polydispersity of Primary Particles in Agglomerates Made by Coagulation and Sintering. *J. Aerosol Sci.*, 38(1):17–38, 2007. doi:10.1016/j.jaerosci.2006.09.005.

[19] D. L. Hildenbrand. Low-Lying Electronic Sates and Revised Thermochemistry of TiCl, $TiCl_2$, and $TiCl_3$. *J. Phys. Chem. A*, 113(8):1472–1474, 2009. doi:10.1021/jp807913c.

[20] International Union of Pure and Applied Chemistry. InChI: Open-Source Chemical Structure Representation Algorithm. Technical FAQ, InChI Trust, 2014. URL `http://www.inchi-trust.org/technical-faq/`.

[21] B. Karlemo, P. Koukkari, and J. Paloniemi. Formation of Gaseous Intermediates in Titanium(IV) Chloride Plasma Oxidation. *Plasma Chem. Plasma Process.*, 16(1): 59–77, 1996. doi:10.1007/BF01465217.

[22] I. J. Krchma and H. H. Schaumann. Production of Titanium Dioxide. US Patent 2,559,638, July 10 1951.

[23] M. L. Laury and A. K. Wilson. Performance of Density Functional Theory for Second Row (4d) Transition Metal Thermochemistry. *J. Chem. Theory. Comput.*, 9(9):3939–3946, 2013. doi:10.1021/ct400379z.

[24] T. J. Lee, C. M. Rohlfing, and J. E. Rice. An Extensive *Ab Initio* Study of the Structures, Vibrational Spectra, Quadratic Force Fields, and Relative Energetics of Three Isomers of Cl_2O_2. *J. Chem. Phys.*, 97(9):6593–6605, 1992. doi:10.1063/1.463663.

[25] W.-K. Li and C.-Y. Ng. Gaussian-2 *Ab Initio* Study of Isomeric Cl_2O_2 and $Cl_2O_2^+$ and Their Dissociation Reactions. *J. Phys. Chem. A*, 101(2):113–115, 1997. doi:10.1021/jp962253d.

[26] W.-K. Li, K.-C. Lau, C. Y. Ng, H. Baumgärtel, and K. M. Weitzel. Gaussian-2 and Gaussian-3 Study of the Energetics and Structures of Cl_2O_n and Cl_2O_n+, n = $1-7$. *J. Phys. Chem. A*, 104(14):3197–3203, 2000. doi:10.1021/jp993398y.

[27] P. J. Linstrom and W. G. Mallard, editors. *NIST Chemistry WebBook, NIST Standard Reference Database Number 69*. National Institute of Standards and Technology (NIST), Gaithersburg MD, 20899, 2005. Retrieved May 13, 2016.

[28] A. McNaught. The IUPAC International Chemical Identifier: InChI - A New Standard for Molecular Informatics. *Chem. Int.*, 28(6):12–15, 2006.

[29] D. McQuarrie and J. Simon. *Molecular Thermodynamics*. University Science Books, Sausalito, CA, United States, 1999. ISBN 9781891389054.

[30] M. Mehta, Y. Sung, V. Raman, and R. O. Fox. Multiscale Modeling of TiO_2 Nanoparticle Production in Flame Reactors: Effect of Chemical Mechanism. *Ind. Eng. Chem. Res.*, 49(21):10663–10673, 2010. doi:10.1021/ie100560h.

[31] M. Mehta, R. O. Fox, and P. Pepiot. Reduced Chemical Kinetics for the Modeling of TiO_2 Nanoparticle Synthesis in Flame Reactors. *Ind. Eng. Chem. Res.*, 54(20): 5407–5415, 2015. doi:10.1021/acs.iecr.5b00130.

[32] J. P. Merrick, D. Moran, and L. Radom. An Evaluation of Harmonic Vibrational Frequency Scale Factors. *J. Phys. Chem. A*, 111(45):11683–11700, 2007. doi:10.1021/jp073974n.

[33] N. Morgan, C. Wells, M. Kraft, and W. Wagner. Modelling Nanoparticle Dynamics: Coagulation, Sintering, Particle Inception and Surface Growth. *Combust. Theor. Model.*, 9(3):449–461, 2005. doi:10.1080/13647830500277183.

[34] N. Morgan, C. G. Wells, M. J. Goodson, M. Kraft, and W. Wagner. A New Numerical Approach for the Simulation of the Growth of Inorganic Nanoparticles. *J. Comput. Phys.*, 211(23):638–658, 2006. doi:10.1016/j.jcp.2005.04.027.

[35] K. Nakaso, T. Fujimoto, T. Seto, M. Shimada, K. Okuyama, and M. M. Lunden. Size Distribution Change of Titania Nano-Particle Agglomerates Generated by Gas Phase Reaction, Agglomeration, and Sintering. *Aerosol Sci. Technol.*, 35(5):929–947, 2001. doi:10.1080/02786820126857.

[36] S. L. Nickolaisen, R. R. Friedl, and S. P. Sander. Kinetics and Mechanism of the Chlorine Oxide ClO + ClO Reaction: Pressure and Temperature Dependences of the Bimolecular and Termolecular Channels and Thermal Decomposition of Chlorine Peroxide. *J. Phys. Chem.*, 98(1):155–169, 1994. doi:10.1021/j100052a027.

[37] D. Nurkowski, P. Buerger, J. Akroyd, and M. Kraft. A Detailed Kinetic Study of the Thermal Decomposition of Tetraethoxysilane. *Proc. Combust. Inst.*, 35(2):2291–2298, 2015. doi:10.1016/j.proci.2014.06.093.

[38] N. M. O'Boyle, M. Banck, C. A. James, C. Morley, T. Vandermeersch, and G. R. Hutchison. Open Babel: An Open Chemical Toolbox. *J. Cheminform.*, 3(1):1–14, 2011. doi:10.1186/1758-2946-3-33.

[39] S. H. Park and S. N. Rogak. A One-Dimensional Model for Coagulation, Sintering, and Surface Growth of Aerosol Agglomerates. *Aerosol Sci. Technol.*, 37(12):947–960, 2003. doi:10.1080/02786820300899.

[40] J. A. Pople, L. Radom, and W. J. Hehre. Molecular Orbital Theory of the Electronic Structure of Organic Compounds. VII. Systematic Study of Energies, Conformations, and Bond Interactions. *J. Am. Chem. Soc.*, 93(2):289–300, 1971. doi:10.1021/ja00731a001.

[41] J. A. Pople, M. J. Frisch, B. T. Luke, and J. S. Binkley. A Møller-Plesset Study of the Energies of AHn Molecules (A = Li to F). *Int. J. Quantum Chem.*, 24(S17):307–320, 1983. doi:10.1002/qua.560240835.

[42] S. E. Pratsinis and P. T. Spicer. Competition Between Gas Phase and Surface Oxidation of $TiCl_4$ During Synthesis of TiO_2 Particles. *Chem. Eng. Sci.*, 53(10):1861–1868, 1998. doi:10.1016/S0009-2509(98)00026-8.

[43] S. E. Pratsinis, H. Bai, P. Biswas, M. Frenklach, and S. V. R. Mastrangelo. Kinetics of Titanium(IV) Chloride Oxidation. *J. Am. Ceram. Soc.*, 73(7):2158–2162, 1990. doi:10.1111/j.1151-2916.1990.tb05295.x.

[44] E. Rühl, U. Rockland, H. Baumgärtel, O. Lösking, M. Binnewies, and H. Willner. Photoionization Mass Spectrometry of Chlorine Oxides. *Int. J. Mass Spectrom.*, 185–187:545–558, 1999. doi:10.1016/S1387-3806(98)14137-4.

[45] H. H. Schaumann. Production of Titanium Oxide Pigments. US Patent 2,488,439, Nov. 19 1949.

[46] J. M. Seddon and J. D. Gale. *Thermodynamics and Statistical Mechanics*. The Royal Society of Chemistry, Cambridge, United Kingdom, 2001. ISBN 978-0-85404-632-4. doi:10.1039/9781847552181-00077.

[47] R. Shirley, Y. Liu, T. S. Totton, R. H. West, and M. Kraft. First-Principles Thermochemistry for the Combustion of a $TiCl_4$ and $AlCl_3$ Mixture. *J. Phys. Chem. A*, 113 (49):13790–13796, 2009. doi:10.1021/jp905244w.

[48] R. Shirley, J. Akroyd, L. A. Miller, O. R. Inderwildi, U. Riedel, and M. Kraft. Theoretical Insights Into the Surface Growth of Rutile TiO_2. *Combust. Flame*, 158(10): 1868–1876, 2011. doi:10.1016/j.combustflame.2011.06.007.

[49] J. Sicre and C. Cobos. Thermochemistry of the Higher Chlorine Oxides ClO_x (x=3, 4) and Cl_2O_x (x=3-7). *J. Mol. Struc.-THEOCHEM*, 620(2–3):215–226, 2003. doi:10.1016/S0166-1280(02)00602-4.

[50] P. T. Spicer, O. Chaoul, S. Tsantilis, and S. E. Pratsinis. Titania Formation by $TiCl_4$ Gas Phase Oxidation, Surface Growth and Coagulation. *J. Aerosol Sci.*, 33(1):17–34, 2002. doi:10.1016/S0021-8502(01)00069-6.

[51] S. M. Tekarli, M. L. Drummond, T. G. Williams, T. R. Cundari, and A. K. Wilson. Performance of Density Functional Theory for 3d Transition Metal-Containing Complexes: Utilization of the Correlation Consistent Basis Sets. *J. Phys. Chem. A*, 113 (30):8607–8614, 2009. doi:10.1021/jp811503v.

[52] T. S. Totton, R. Shirley, and M. Kraft. First-Principles Thermochemistry for the Combustion of $TiCl_4$ in a Methane Flame. *Proc. Combust. Inst.*, 33(1):493–500, 2011. doi:10.1016/j.proci.2010.05.011.

[53] S. Tsantilis and S. E. Pratsinis. Narrowing the Size Distribution of Aerosol-Made Titania by Surface Growth and Coagulation. *J. Aerosol Sci.*, 35(3):405–420, 2004. doi:10.1016/j.jaerosci.2003.09.006.

[54] U.S. Department of the Interior and U.S. Geological Survey. National Minerals Information Center, 2016. URL `http://http://minerals.usgs.gov/minerals/`. Retrieved August 29, 2016.

[55] T.-H. Wang, A. M. Navarrete-López, S. Li, D. A. Dixon, and J. L. Gole. Hydrolysis of $TiCl_4$: Initial Steps in the Production of TiO_2. *J. Phys. Chem. A*, 114(28):7561–7570, 2010. doi:10.1021/jp102020h.

[56] D. Weininger. SMILES, a Chemical Language and Information System. 1. Introduction to Methodology and Encoding Rules. *J. Chem. Inform. Comput. Sci.*, 28(1): 31–36, 1988.

[57] D. Weininger, A. Weininger, and J. L. Weininger. SMILES. 2. Algorithm for Generation of Unique SMILES Notation. *J. Chem. Inform. Comput. Sci.*, 29(2):97–101, May 1989. doi:10.1021/ci00062a008.

[58] R. H. West, G. J. O. Beran, W. H. Green, and M. Kraft. First-Principles Thermochemistry for the Production of TiO_2 from $TiCl_4$. *J. Phys. Chem. A*, 111(18):3560–3565, 2007. doi:10.1021/jp0661950.

[59] R. H. West, M. S. Celnik, O. R. Inderwildi, M. Kraft, G. J. O. Beran, and W. H. Green. Toward a Comprehensive Model of the Synthesis of TiO_2 Particles from $TiCl_4$. *Ind. Eng. Chem. Res.*, 46(19):6147–6156, 2007. doi:10.1021/ie0706414.

[60] R. H. West, R. A. Shirley, M. Kraft, C. F. Goldsmith, and W. H. Green. A Detailed Kinetic Model for Combustion Synthesis of Titania from $TiCl_4$. *Combust. Flame*, 156 (9):1764–1770, 2009. doi:10.1016/j.combustflame.2009.04.011.

Citation index

Abramowitz and Chase [1], 10
Akroyd et al. [2], 4
Atkinson et al. [3], 10
Bloss et al. [4], 10
Boese et al. [5], 7
Buerger et al. [6], 5, 7, 9
Buerger et al. [7], 10–12
Buerger et al. [8], 15
Buerger et al. [9], 10, 11
Chase [10], 10, 12
DeMore et al. [11], 10
Frisch et al. [12], 7
Ge et al. [13], 7
Ghoshtagore [14], 3
Goodwin [15], 12
Hanson-Heine et al. [16], 7
Hehre et al. [17], 9
Heine and Pratsinis [18], 3
Hildenbrand [19], 10, 12
International Union of Pure and Applied Chemistry [20], 4
Karlemo et al. [21], 13
Krchma and Schaumann [22], 3
Laury and Wilson [23], 7
Lee et al. [24], 10
Li and Ng [25], 10
Li et al. [26], 10
Linstrom and Mallard [27], 10, 12
McNaught [28], 4
McQuarrie and Simon [29], 9
Mehta et al. [30], 4
Mehta et al. [31], 4
Merrick et al. [32], 7
Morgan et al. [33], 3
Morgan et al. [34], 3
Nakaso et al. [35], 4
Nickolaisen et al. [36], 10
Nurkowski et al. [37], 15
O'Boyle et al. [38], 4, 7
Park and Rogak [39], 4
Pople et al. [40], 9
Pople et al. [41], 9
Pratsinis and Spicer [42], 3, 4
Pratsinis et al. [43], 3, 4
Rühl et al. [44], 10
Schaumann [45], 3
Seddon and Gale [46], 9
Shirley et al. [47], 3
Shirley et al. [48], 4
Sicre and Cobos [49], 10
Spicer et al. [50], 4
Tekarli et al. [51], 7
Totton et al. [52], 3
Tsantilis and Pratsinis [53], 3, 4
Wang et al. [55], 10, 12
Weininger et al. [57], 4
Weininger [56], 4
West et al. [58], 3–5, 11, 12, 14, 15
West et al. [59], 3, 15
West et al. [60], 3–5, 11, 13, 15
U.S. Department of the Interior and U.S. Geological Survey [54], 3